PROTEINS: Structure, Function, and Genetics 32:414–424 (1998)

Recognition of Single-Stranded DNA by Nuclease P1: High Resolution Crystal Structures of Complexes With Substrate Analogs

Christophe Romier,[1] Roberto Dominguez,[2] Armin Lahm,[3] Otto Dahl,[4] and Dietrich Suck[1]*
[1]*European Molecular Biology Laboratory, Heidelberg, Germany*
[2]*Rosenstiel Basic Medical Science Research Center, Brandeis University, Waltham, Massachusetts*
[3]*Istituto di Ricerche di Biologia Molecolare P. Angeletti, Pomezia, Italy*
[4]*Department of General and Organic Chemistry, University of Copenhagen, Copenhagen, Denmark*

ABSTRACT **The reaction mechanism of nuclease P1 from *Penicillium citrinum* has been investigated using single-stranded dithiophosphorylated di-, tetra-, and hexanucleotides as substrate analogs. The complexes crystallize in tetragonal and orthorhombic space groups and have been solved by molecular replacement. The high resolution structures give a clear picture of base recognition by P1 nuclease at its two nucleotide-binding sites, especially the 1.8 Å structure of a P1-tetranucleotide complex which can be considered a P1-product complex. The observed binding modes are in agreement with a catalytic mechanism where the two closely spaced zinc ions activate the attacking water while the third, more exposed zinc ion stabilizes the leaving 03' oxyanion. Stacking as well as hydrogen bonding interactions with the base 5' to the cleaved phosphodiester bond are important elements of substrate binding and recognition. Modelling of a productive P1-substrate complex based on the solved structures suggests steric hindrance as the likely reason for the resistance of Rp-phosphorothioates and phosphorodithioates. Differences with the highly homologous nuclease S1 from *Aspargillus oryzae* are discussed. Proteins 32:414–424, 1998.**

Key words: P1 nuclease; X-ray crystallography; substrate recognition; catalytic mechanism; thiophosphorylated oligonucleotides

INTRODUCTION

P1 nuclease from Penicillium citrinum is a 36 kDa glycoprotein which degrades single-stranded RNA and DNA.[1–4] The enzyme is a phosphodiesterase cleaving the P-O3′ bond with inversion of configuration at the phosphorus,[5] but also acts as a phosphomonoesterase removing 3′-terminal phosphate groups.[1,2]

P1 is unable to cleave phosphodiester bonds with an abasic 5′-nucleotide, whereas removal of the base of the 3′-nucleotide does not affect hydrolysis.[6] Using ring-saturated base analogs it was shown that the aromaticity of the 5′-base affects the activity indicating that it may be involved in a stacking interaction with an aromatic protein side chain.[7] The importance of the 5′-base for P1 activity was reinforced by the finding that, although P1 is essentially unspecific, the enzyme shows some dependence of its cleavage rates on the identity of the base 5′ to the cleaved bond.[8]

P1 nuclease is a zinc-dependent enzyme containing three zinc ions per monomer.[4] The crystal structure revealed that the zinc ions are bound in a pocket forming the active site which is not accessible for regular double-stranded substrates.[9,10] Two of the zinc ions form a closely spaced dinuclear pair and are buried at the bottom of the pocket, whereas the third ion is further apart and more solvent exposed. Surprisingly, the three-dimensional structure of P1 was found to be closely related to the structure of *Bacillus cereus* phospholipase C (PLC) with almost identical disposition and coordination of the three zinc ions.[11]

The R-diastereomers of monothiophosphorylated oligonucleotides are resistant to P1 nuclease treatment, whereas the S-diastereomers are cleaved at somewhat reduced rates compared to the unmodified substrates.[5, 12] Analysis at low resolution of P1 crystals soaked with the R-diastereomer of the monothiophosphorylated dinucleotide d[Ap(S)A] (R-Ap(S)A) revealed two mononucleotide binding sites 20 Å apart[10] (Fig. 1). The first site (Phe-site) is located close to the three zinc ions in the active site, with the adenine base stacked against the side chain of Phe61. At the bottom of this binding site, the carboxylate of Asp63 is in hydrogen bonding distance of the N1 and the 6-NH2 positions of the adenine. At the second binding site (Tyr-site), an adenine is sandwiched between Tyr144 and Tyr155 and forms

*Correspondence to: Dietrich Suck, European Molecular Biology Laboratory, Meyerhofstrasse 1, 69017 Heidelberg, Germany. E-mail: suck@embl-heidelberg.de
Received 22 December 1997; Accepted 28 April 1998

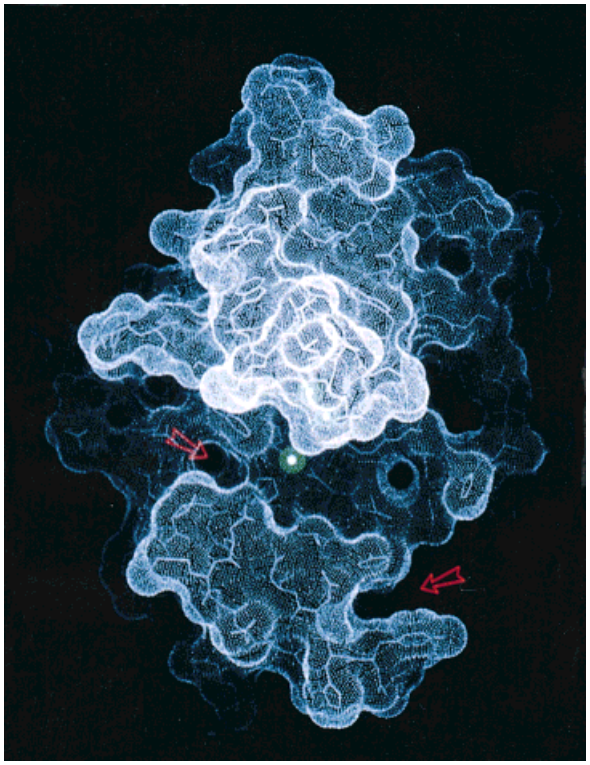

Fig. 1. Nucleotide binding pockets of P1. The van der Waals surface of P1 highlights the two hydrophobic nucleotide binding pockets (indicated by red arrows) which are formed by residues Phe61/Val132 (**left**) and Tyr144/Tyr155 (**right**). A channel linking the two sites is clearly seen. Zinc ions are displayed as green spheres with a white dot in the center: Zn2, the more exposed zinc ion, is clearly visible, whereas the binuclear pair formed by Zn1 and Zn3 is buried within the protein and therefore hardly visible.

similar interactions with Asp146 carboxylate at the bottom of the pocket. This second site is missing in the closely related S1 nuclease from *Aspergillus oryzae*[13].

Although the soaking experiment with R-Ap(S)A provided evidence for two nucleotide binding sites in P1, major questions concerning the reaction mechanism remained unanswered, especially due to the low resolution of the structure of the complex (3.0 Å) which rendered the interpretation difficult. At both sites only mononucleotides could be built into the electron density suggesting that either the dinucleotide is cleaved or partially disordered. The former is unlikely since no cleavage of R-Ap(S)A could be detected under crystallization conditions and binding of 5'-AMP, an inhibitor of the enzyme, leads to a distinctly different position for the phosphate moiety centered between the three zincs as shown in a separate soaking experiment (A. Lahm and D. Suck, unpublished results). While the nucleotide density at the active site of the P1-(R-Ap(S)A) complex appeared to be somewhat more consistent with a bound 3'-half of the dinucleotide, the analysis at 3 Å resolution did not allow to unambiguously define the orientation of the R-Ap(S)A and leaves open the possibility of multiple, non-productive binding modes.

Based on these crystallographic results several possible reaction mechanisms can be envisaged. All of these involve nucleophilic attack by a zinc activated water molecule and stabilization of the pentacovalent transition state by Arg48, but assign different roles to the three zinc ions and the firmly bound water molecules seen in the P1 crystal structure.[10] In one mechanism, the more exposed Zn2 activates a nearby water molecule, possibly assisted by an aspartate residue (Asp153), while the dinuclear, cocatalytic zinc pair (Zn1 and Zn3)[14] plays a more passive role.[10] In a second mechanism, the water bridging the buried Zn1 and Zn3 ions is activated and acts as the attacking nucleophile, while Zn2 is activating and stabilizing the O3′-leaving group.[15] In a third mechanism, analogous to the two-metal ion mechanism proposed for the 3′,5′-exonuclease activity of *E. coli* DNA polymerase I,[16,17] it is assumed that one of the non-bridging phosphate oxygens binds between Zn1 and Zn3, replacing the bridging water molecule.

We have further investigated the reaction mechanism of P1 by cocrystallization experiments with thiophosphorylated substrate analogs. In order to avoid any risk of cleavage we have used dithiophosphorylated oligonucleotides which are completely resistant against P1 treatment (C. Romier and D. Suck, unpublished data). The structures of several complexes with modified oligonucleotides varying in length between 2 and 6 nucleotides were solved by molecular replacement. Although none of the substrate analogs binds in a productive way, the high resolution structures provide a detailed picture on how P1 nuclease recognizes nucleotides. In addition, one of them can be considered an enzyme-product complex and is consistent with a reaction mechanism involving nucleophilic attack by the water molecule bridging the dinuclear zinc pair.

MATERIAL AND METHODS

Crystallization

P1 nuclease was purchased from Sigma and dissolved in a buffer composed of 25 mM sodium acetate pH 5.3, 2 mM zinc chloride to reach a protein concentration of 1 mM. All dithionucleotides were synthesized in the laboratory of O. Dahl[18] and dissolved in water to reach a concentration of 10 mM. Prior to crystallization, the protein and the DNA solutions were mixed to obtain a DNA/protein ratio of 2, the final protein concentration being 0.8 mM. Three dithiophosphorylated oligonucleotides were used: d[A(pS2)T], d[A(pS2)T(pS2)T(pS2)T] and d[A(pS2)T(pS2)A(pS2)A(pS2)A(pS2)A] (called AT, ATTT, and ATAAAA, respectively).

Crystals were grown in hanging drops by vapor diffusion in Linbro plates (ICN Pharmaceuticals Inc., Costa Mesa, CA). Droplets were formed by mixing 1 µl of protein/DNA solution with 1 µl of

reservoir solution. Reservoir solutions were composed of 25 mM sodium acetate pH 5.3 and polyethyleneglycol 6000 ranging from 12 to 20% (w/v). In some crystallisation conditions, zinc chloride was also added to the reservoir to reach a concentration of 2 mM. Crystals grew within one night to one week depending on the complex crystallized.

When zinc chloride was added to the reservoir before mixing, the crystals were easily reproducible. Under these conditions, crystals for all three complexes were obtained, although the P1-ATAAAA complex crystals did not diffract. The two other complexes crystallised in tetragonal space group (P41212, Table I). When no zinc was added to the reservoir, crystals could not be easily reproduced. Again, the three complexes gave crystals, tetragonal as those obtained without zinc for the P1-AT complex, but orthorhombic (space group P212121) for the two other complexes (Table I).

The reason for obtaining different space groups is unclear. In both cases a zinc ion is found at the interface of two symmetry-related molecules. When the zinc is only provided by the protein buffer (orthorhombic case for the ATTT and ATAAAA oligonucleotides), it seems that its concentration is not high enough in the droplet and the DNA becomes the crystallization driving force by linking symmetry-related molecules. This is not true for the AT nucleotide, possibly due to its small size, which only gives tetragonal crystals (rather seldom when the zinc concentration is low).

Data Collection and Processing

All diffraction data were collected at room temperature on a MAR-research image plate system with CuK α X-rays generated by an Enraf-Nonius rotating anode generator operating at 40 kV and 90 mA, equipped with a graphite monochromator. All data were processed using XDS.[19] Data statistics are summarized in Table II.

Molecular Replacement and Structure Refinement

A search model for molecular replacement was generated from the 2.8 Å resolution structure of P1.[10] This starting model included residues 1 to 269 and the three zinc ions forming the active site. Molecular replacement solutions were obtained with AMORE[20] using data from 10 to 3 Å resolution. For all three complexes a single solution peak around 70 σ was obtained in the rotation and translation searches. Subsequent rigid-body refinement in AMORE improved the R-factors for these solutions from initially around 35 to about 30%.

The complex structures were refined using X-PLOR[21], with Engh and Huber[22] parameters, by several cycles of Powell minimization and manual

TABLE I. Crystal Data of the P1 Complexes

Complex	P1-AT	P1-ATTT		P1-ATAAAA
Space group	$P4_12_12$	$P4_12_12$	$P2_12_12_1$	$P2_12_12_1$
a (Å)	77.2	77.4	42.0	41.5
b (Å)	77.2	77.4	74.0	72.8
c (Å)	156.6	157.0	102.1	101.1
Resolution (Å)	2.2	2.9	1.8	2.1

TABLE II. Data Statistics

Complex	P1-AT	P1-ATTT		P1-ATAAAA
Space group	$P4_12_12$	$P4_12_12$	$P2_12_12_1$	$P2_12_12_1$
Resolution (Å)	2.2	2.9	1.8	2.1
Number of observations	157682	90863	119199	68514
Unique reflections	24294	10848	27854	17665
Completeness (%)				
Overall	97.8	96.9	93.2	95.4
Last shell[a]	99.0	74.2	89.9	96.6
R_{sym}[b] (%)				
Overall	7.3	7.4	6.8	10.4
Last shell[a]	23.9	15.8	24.7	37.5

[a]The last shells for the four complexes are 2.3–2.2 Å, 3.0–2.9 Å, 1.95–1.80 Å, and 2.15–2.1 Å, respectively.
[b]The R_{sym} value is indicated without any sigma cutoff.

TABLE III. Refinement Statistics of the Complexes

Complex	P1-AT	P1-ATTT[a]	P1-ATAAAA
Space group	$P4_12_12$	$P2_12_12_1$	$P2_12_12_1$
Resolution range (Å)	8.0–2.2	8.0–1.8	8.0–2.1
Number of protein atoms (non-hydrogen)	2032	2022	2022
Number of sugar atoms (non-hydrogen)	28[c]	56[c]	39[c]
Number of zinc atoms	4[d]	4[d]	4[d]
Number of DNA atoms (non-hydrogen)	22[e]	78	0[e]
Number of water molecules	205	153	105
R-factor (%)	17.9	20.7	21.1
R-free[b] (%)	21.3	23.5	25.7
Deviations from ideal geometry			
Bonds (Å)	0.010	0.011	0.013
Angles (°)	1.57	1.70	1.75
Mean temperature factor (Å^2)	27.1	21.8	21.2

[a]The structure of the P1-ATTT complex in space group $P4_12_12$ was not refined (see text).
[b]The R-free was calculated from a random selection of reflections constituting ~10% of the data.[23]
[c]The sugar atoms correspond to the carbohydrate side chains. The differences between the complexes are due to the number of sugar units which could be built in the electron density.
[d]A fourth zinc ion is always found at the interface between two symmetry-related molecules and seems to be important for crystallization.
[e]For these two complexes, the oligonucleotides were not built or were only partially built due to ambiguous portions of electron density.

corrections. A random selection of 10% of the data was used for the calculation of the Rfree[23]. All model building was carried out within TURBO-FRODO[24]. The quality of the refined structures was estimated using X-PLOR and PROCHECK[25]. Overall refinement statistics are given in Table III.

Due to the ambiguities in building the dithiophosphorylated oligonucleotides into the electron density of most of the complexes, only the P1-ATTT complex has been submitted to the Protein Data Bank where it has been given the ID code 1ak0. All other structures are available from the authors upon request.

RESULTS

Choice of the Substrate Analogs and Cocrystallization

Inspecting the accessible surface of nuclease P1 in the vicinity of both nucleotide-binding sites reveals a channel connecting both sites (Fig. 1). This prompted us to use tetra- and hexanucleotides for cocrystallization experiments which were expected to bind in the channel spanning the two binding sites. Dithiophosphorylated oligonucleotides were chosen as substrate analogs because of their resistance to P1. By HPLC analysis we could show that they are stable under crystallization conditions, i.e. in the presence of large amounts of P1 (data not shown). Three oligonucleotides were designed which have been termed AT, ATTT, and ATAAAA (see Material and Methods). Under similar crystallization conditions the ATTT oligonucleotide in complex with P1 gave both orthorhombic and tetragonal crystals, whereas ATAAAA gave only orthorhombic, and AT only tetragonal crystals (Table I). The diffraction limit of the crystals varied between 2.9 and 1.8Å and decreased in both space groups with increasing length of the oligonucleotides. The best resolution obtained, which is also the best resolution ever obtained for a P1 crystal, was 1.8 Å with the orthorhombic P1-ATTT complex.

Overall Structures of the Complexes

The differences observed between the two crystal forms are mainly due to the oligonucleotide binding. In the orthorhombic form, one oligonucleotide molecule links two symmetry-related molecules. In the orthorhombic P1-ATTT complex, the adenine is bound in the Tyr-site of one P1 molecule, and the 3′-terminal thymine is bound in the Phe-site of a second, symmetry-related P1 molecule (Fig. 2a). The two central thymines are not specifically recognized by any protein side-chain and their electron density in the 2Fo - Fc map is less well defined, although a large part of the backbone, especially the phosphates, is clearly visible (Fig. 2b). In the P1-ATAAAA complex, apparently two adjacent nucleotides form the link between both molecules, explaining the smaller cell constants observed (Table I). The density for these nucleotides in this complex is not as clear as in the ATTT complex, and it is not possible to distinguish which part of the hexanucleotide is bound and in which orientation.

The tetragonal P1-AT and P1-ATTT cocrystals display a totally different picture. In both complexes, density for the oligonucleotide is only seen at both nucleotide-binding sites with no evidence for cross-linking either within or between molecules, and an adenine is always found at the Tyr-site. At the Phe-site however, the density is not interpretable, presumably due to the binding of the oligonucleotide in different orientations.

Overall, the P1 structures seen in the various complexes are nearly identical to the nucleotide-free enzyme. However, some changes are observed in the vicinity of the active site even though no changes are seen in the zinc positions and their coordinating side-chains. For instance, a slight increase of the B-values of the atoms of the loop formed by residues Tyr47 to Thr50 is observed, and indicates some flexibility. Additionally, the side chain of Arg48 is found in several conformations in the complexes. Drastic changes are seen in the orientation of the side chain of Phe61 that seem to be crucial for the required flexibility in substrate recognition (Fig. 3). Such large variations are not observed at the Tyr-site where only small movements are seen for Tyr144 and Tyr155. The more rigid binding pocket is possibly the reason why the nucleotide density at the Tyr-site is normally better defined than at the Phe-site.

Base Recognition at the Tyr-site

In most of the complexes, an adenine is bound at the Tyr-site although the difference density in the P1-ATAAAA complex does not allow to unambiguously decide whether an adenine or a thymine is bound. In all complexes tight stacking contacts are formed between the base and the tyrosine rings of Y144 and Y155 (Fig. 2a,c). Recognition of the adenine is mediated through a bidentate hydrogen bonding contact with Asp146 at the bottom of the pocket involving the 6-NH2 group and nitrogen N1, as previously described for the P1-(R-Ap(S)A) complex.[10] The latter contact however requires either a protonation at N1—which is a reasonable assumption given the pH of crystallization (5.3), which is also the optimum pH for P1 activity—or a protonation of the aspartate, which is also possible given the hydrophobic nature of the binding pocket. Additional evidence for the protonation of Asp146 is its direct interaction with the carboxylate group of Asp151 as found in the native structure.[10]

Base Recognition at the Phe-site

The crystal structures of the different complexes described in this paper have provided clues on how both adenine and thymine are recognized at the Phe-site, i.e., at the active site of the enzyme. As

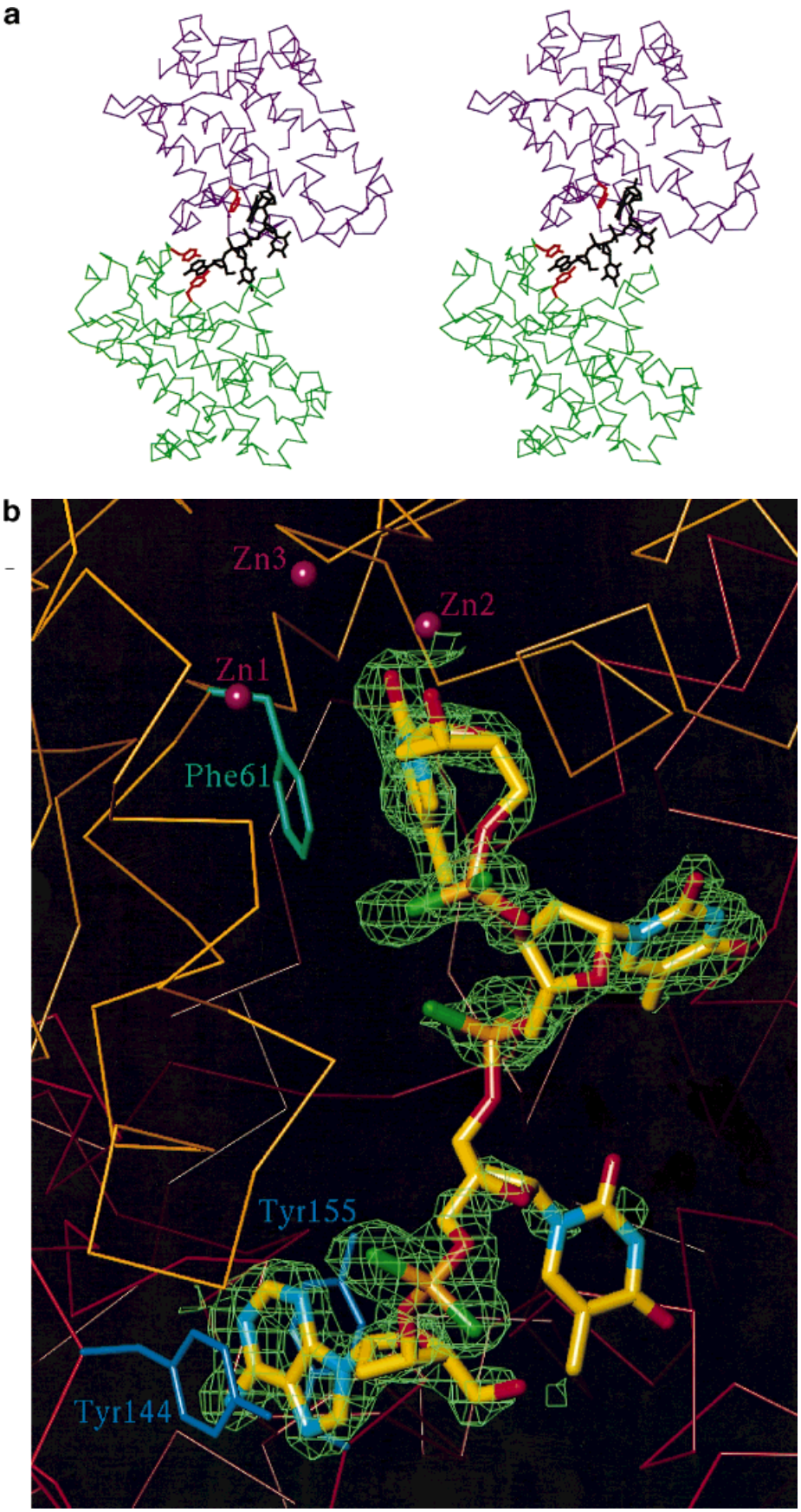

Fig. 2. Orthorhombic P1-ATTT complex. (**a**) Stereo representation of the P1-ATTT complex. Shown are the Cα-positions of two neighbouring P1 molecules (green and purple) 'cross-linked' by the ATTT tetranucleotide (black). The 5′-terminal adenine is stacked between Tyr144 and Tyr155 ('Tyr-site', red side-chains of green molecule) of the first molecule, while the 3′-terminal thymidine is bound at the active site of the neighbouring molecule stacking against Phe61 ('Phe-site', red side-chain of purple molecule). (**b**) 2Fo-Fc electron density contoured at 1.5 σ of the ATTT molecule in the orthorhombic form of the P1-ATTT complex. The oligonucleotide cross-links two symmetry-related molecules. (**c**) 2Fo-Fc electron density map contoured at 1.5 s of the adenine bound in the Tyr-site of the orthorhombic P1-ATTT complex. (**d**) Stereo representation of the 2Fo-Fc electron density of the 3′-terminal thymidine showing the orientation of the deoxyribose and in particular of the 3′-hydroxyl group relative to the zinc cluster.

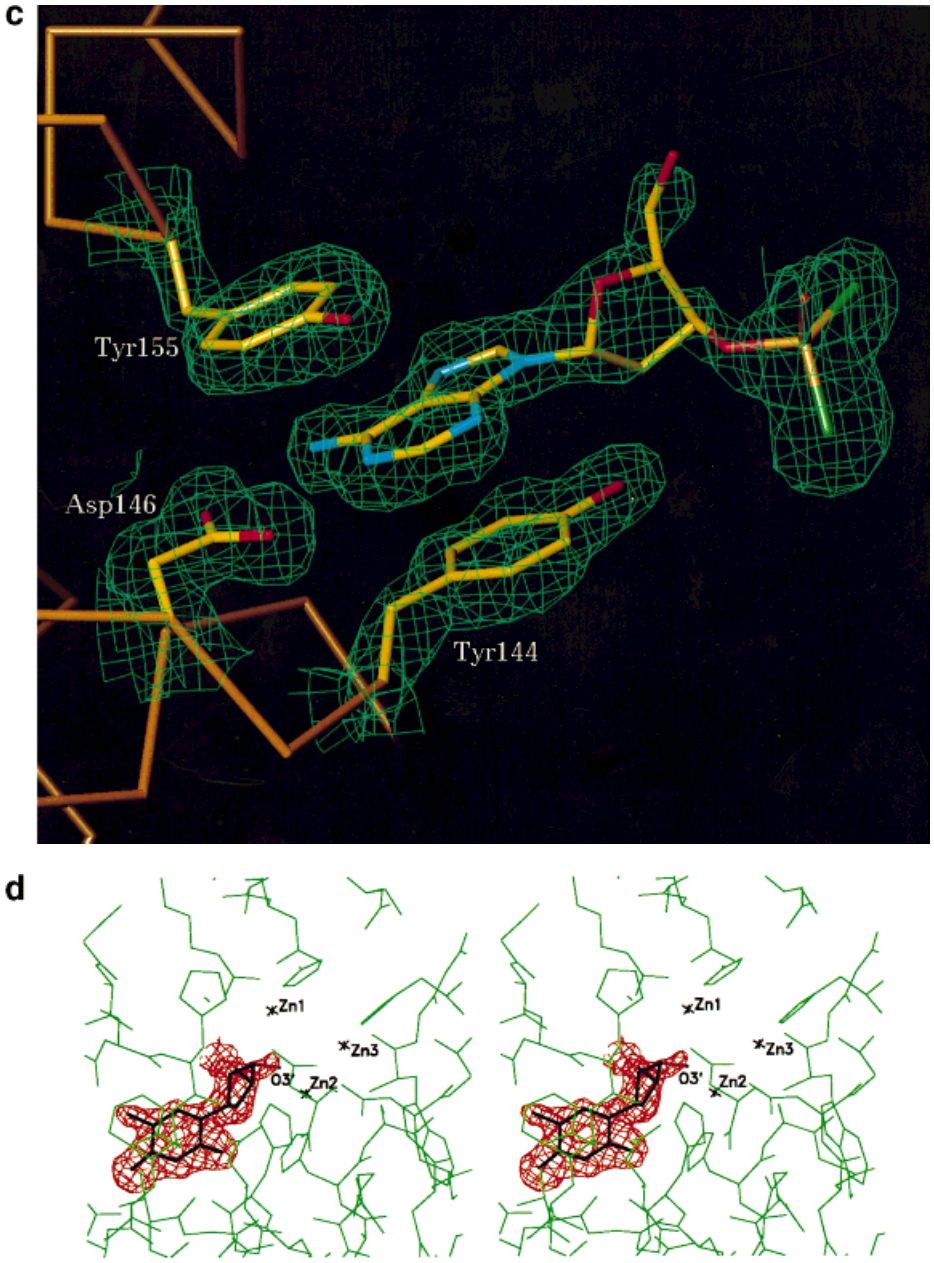

Figure 2. (Continued.)

mentioned above, the previously solved P1-(R-Ap(S)A) complex suggested that adenine recognition at this site involves hydrogen bonding of the 6-NH2 group and N1 with Asp63 at the bottom of the pocket (Fig. 4a). Like at the Tyr-site, this requires protonation of either N1 or the carboxylate. The density for the P1-AT and P1-ATAAAA complexes is not of sufficient quality to show any details of the interactions at the Phe-site.

A much clearer picture is provided for the binding of thymine at the Phe-site in the orthorhombic ATTT complex (Figs. 2a,d and 4b). The 3′-terminal thymine forms a stacking contact with Phe61 and its O4 oxygen is in hydrogen bonding distance (2.8 Å) from one of the oxygens of the Asp63 carboxylate group, again suggesting that this carboxylate is protonated. The O3′ oxygen of the 3′-terminal ribose is coordinating the more exposed zinc ion (Zn2). Both the base and sugar of the 3′-thymidine are firmly bound to the protein as indicated by the well-defined electron density and the low B-factors.

DISCUSSION

Nucleotide Recognition by Nuclease P1

The structures of the dithio-oligonucleotide complexes described in this paper confirm the existence

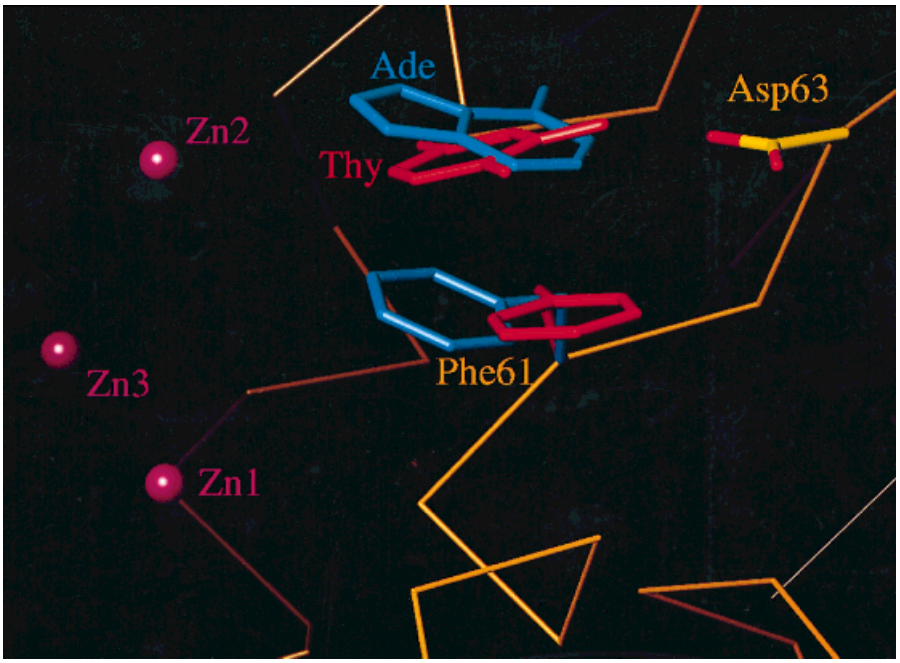

Fig. 3. Adaptation of the active-site binding pocket. The orientation of the phenylalanine ring of Phe61 and the respective bound nucleobase in the R-Ap(S)A (blue) and the ATTT (red) complexes is shown. In both cases optimal base stacking and simultaneous hydrogen bonding contact with Asp63 at the bottom of the binding pocket is achieved by re-orientation of Phe61. The orientation of Phe61 in the P1-ATAAAA complex, as well as in the free protein, is very similar to that seen in the R-Ap(S)A complex.

of two mononucleotide binding sites in P1. At both sites, as previously seen in the P1-(R-Ap(S)A) complex, base recognition involves stacking interactions with exposed aromatic residues as well as hydrogen bonding contacts with carboxylate groups at the bottom of the binding pockets. Stacking interactions have been found in many ss-DNA and RNA binding proteins and can be considered a hallmark of this class of proteins.[26,27] The presence of hydrogen bonds to the bases, on the other hand, may be surprising at first glance for an essentially unspecific nuclease. However, contacts to the functional groups of the bases have been observed in other ss-DNA binding proteins, as for example, in human replication protein A.[28]

Quantitative analysis of P1 hydrolysis patterns of heat-denatured DNA, poly- and dinucleotides revealed certain base preferences and a dependence of the optimal pH for degradation on the sequence.[2,3,8] These observations may at least in part reflect differences in the contacts formed by the various bases in the active site binding pocket (Figure 4). While an adenine could form a bidentate hydrogen bond with the protonated carboxylate, only a single contact is formed with a thymine involving the O4 oxygen. With an unprotonated carboxylate, an adenine could still form the contact to the 6-NH2 group, but no favorable contact would be possible with the thymine (or uracil) O4 position (Fig. 4). On the other hand, simultaneous protonation of adenine N1 and the carboxylate group would be unfavorable. This may contribute to the low pH optimum for P1 hydrolysis of poly U (4.0) compared to poly A (6.0).[2]

The P1 complex structures on the other hand highlight the adaptability of the active site binding pocket: all four types of bases can form at least one hydrogen bond with Asp63, if it is protonated, which is likely at the optimal pH (5.3) for hydrolysis of mixed sequence RNA and DNA (Fig. 4). Furthermore, as can be seen by comparing the P1-(R-Ap(S)A) and P1-ATAAAA structures with the P1-ATTT complex, the binding of different bases is accompanied by a reorientation of Phe61 which enables optimal stacking contacts in each case (Fig. 3).

Less flexibility seems to be present at the Tyr-site where stacking between two tyrosine rings and interaction with Asp146 apparently favors the binding of adenine over thymine. As judged by the crystallographic results, the affinity for the Tyr-site is at least as strong as for the Phe-site, however, the relevance of this site for hydrolysis of substrates is not clear (see below).

We expected that the oligonucleotides would bind along the channel connecting the two nucleotide binding pockets of P1 (Fig. 1). The complex structures solved so far do not provide evidence for this mode of binding or any additional subsites. In the orthorhombic ATTT complex, the tetranucleotide connecting two P1 molecules does not form any contacts to the protein with its two central nucleo-

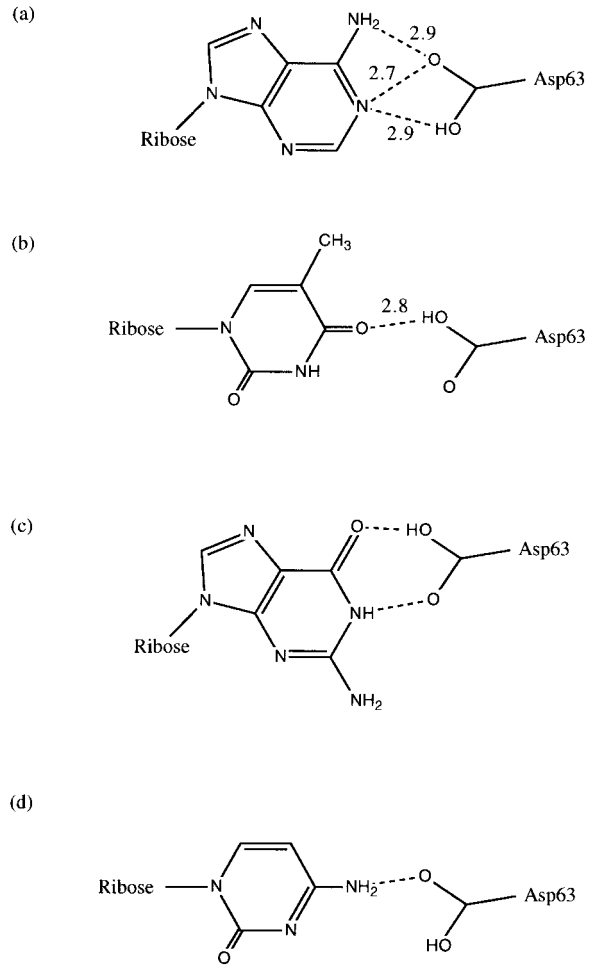

Fig. 4. Base recognition at the active site. Observed (for (**a**) adenine and (**b**) thymine) and proposed (for (**c**) guanine and (**d**) cytosine) hydrogen bonding interaction of the base 5′ to the cleaved phosphodiester bond with Asp63. The observed distances are indicated in Å.

tides. It is likely that this intermolecular binding mode is induced by crystal contacts. However, in the tetragonal form of the ATTT complex, where the intermolecular cross-linking is not possible, no density connecting the two nucleotide binding sites of one molecule is visible either, suggesting that there are no subsites along the channel (data not shown).

Catalytic Mechanism

Crystallographic studies of nuclease-oligonucleotide complexes require the use of either an inactivated enzyme, e.g., an inactive mutant, or of a non-cleavable substrate analog to prevent degradation during the experiment. In both cases a non-productive complex is obtained and it may therefore not be straightforward to draw conclusions about the catalytic mechanism. This general caveat also applies to the dithiosubstituted oligonucleotide complexes described in this paper and the previously reported P1-(R-Ap(S)A) complex. None of these complexes shows directly how the scissile phosphate will be positioned relative to the active site residues and the zinc cluster in a productive complex. However, the 1.8 Å structure of the orthorhombic P1-ATTT complex which can be considered a P1-product complex provides an excellent experimental basis for modelling such a complex.

The 3′-terminal thymidine of ATTT is stacking with its base against Phe61 and its deoxyribose, in particular the O3′ hydroxyl is located close to Zn2, the more exposed zinc ion, replacing one of the strongly bound water molecules seen in the free enzyme (Fig. 2d). This binding is not expected to be influenced by the dithiophosphate groups that lie outside the active site pocket and are not in direct contact with the protein. This suggests that the last thymidine of ATTT is bound to the protein in a natural way and the low B-factors observed for the atoms of both the base and the ribose do support this notion. Such an interaction can be considered as a complex between P1 nuclease and one of its products after cleavage of the O3′-P bond. The other part of the oligonucleotide, being not specifically recognized, would have already departed. If one extends the chain in the 3′ direction, keeping the position of the 3′-terminal thymidine as seen in the complex, the scissile phosphate can occupy a position between the three zinc ions, closest to Zn2, such that the OR non-bridging oxygen replaces a water molecule bound at the active site of P1. This non-bridging oxygen also coordinates Zn2 whereas the other one can form a hydrogen bond with the side chain of R48. This latter residue is also able to form a contact with O5′ (Fig. 5). In this orientation, the O3′-P bond is ideally positioned for an in-line attack by the water bridging Zn1 and Zn3.

This model also provides an explanation for the fact that Sp- but not di- and Rp-thiophosphorylated oligonucleotides are cleaved by nuclease P1. Given the affinity of zinc for sulfur we do not think this is due to the somewhat different charge distribution in the P-S bond, but rather caused by steric hindrance as a consequence of the larger van der Waals radius of sulfur and the longer P-S bond (~1.9 Å as compared to 1.5 Å for a normal P-O bond)[29]. Inspection of our model (Fig. 5) shows, that the sulfur atom of a phosphorothioate group with Rp-configuration (i.e. with a sulfur at position 'OR' in Figure 5) would indeed cause steric interference, particularly with Zn2. In the Sp-diastereomer on the other hand, the sulfur would point to the other side where it could interact with R48. On this side enough space is available to accommodate the larger P-S group without changing the phosphorus and/or zinc positions. For dithio-substituted substrates one would accordingly expect similar, if not even more severe steric interference. This is in agreement with biochemical data showing that phosphorodithioates and Rp-

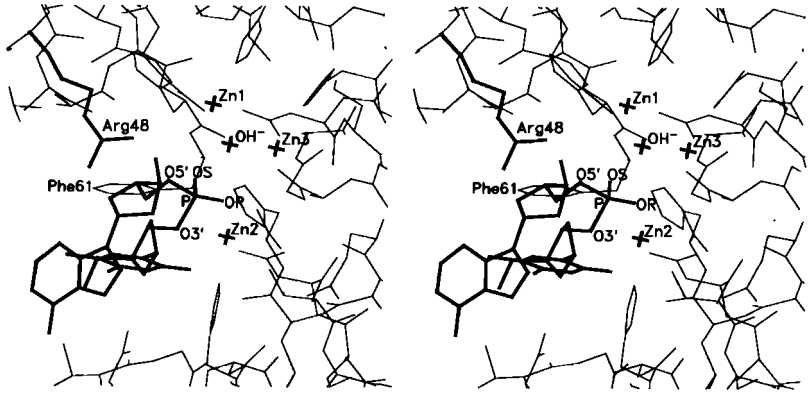

Fig. 5. Proposed productive P1-substrate complex. The productive complex was modelled by extending the bound oligonucleotide of the P1-ATTT complex in the 3′-direction, i.e. the position of the 5′-thymidine including the O3′ oxygen is the same as that of the 3′-terminal thymidine in the ATTT complex. In the position and orientation of the scissile phosphate shown in the figure, the OR and O3′ oxygens replace water molecules (bound to Zn2) present in all substrate-free P1 crystal structures and the water molecule bridging Zn1 and Zn3 (indicated as OH- since it is presumably deprotonated) is optimally positioned for an in-line attack at the phosphorous opposite O3′. For this constellation, the rotation around the O3′-P bond is severely restricted by the zinc ions and their ligands. A sulfur occupying the position of the OR-oxygen would sterically interfere with Zn2, while in an Sp-configuration of the phosphorothioate no steric hindrance is expected and the sulfur (at the position of the OS-oxygen) could interact with R48. This would explain why Sp- but not Rp-phosphorothioates are cleaved by nuclease P1.The orientation of the 3′-nucleoside shown in the figure is arbitrary and only indicates the approximate direction of the oligonucleotide chain.

phosphorothioates are not cleaved by nuclease P1 while Sp-phosphorothioates are cleaved at only slightly reduced rates compared to normal substrates.[5] A rotation around the O3′-P bond is severely restricted since it would create steric clashes between Zn2 and the non-bridging atoms (either oxygen or sulfur), or even steric clashes between the protein and the 3'-nucleotide.

If one would move the phosphate away from the zinc ions by a rotation around the C3′-O3′, these steric constraints would be relieved and, contrary to the biochemical observations, Rp- as well as Sp-phosphorothioates could be cleaved. Furthermore, in this case the water bridging Zn1 and Zn3 would not be able to attack the scissile phosphate, and another water, which has not been identified in the various complexes we solved, would have to play this role.

Based on the model shown in Figure 5, where the scissile phosphate sits between the three zincs, the following mechanism for P1 appears plausible (Fig. 6): the scissile phosphate binds close to Zn2 with its free oxygens replacing two water molecules and the base 5′ to the cleaved bond stacks against Phe61 and forms hydrogen bonding contacts with Asp63. The water molecule bridging Zn1 and Zn3, which like in other binuclear metallohydrolases is presumably present as a hydroxide ion due to the lowering of its pKa by the metal ions,[30,31] acts as the nucleophile attacking the phosphate in-line with the P-O3′ bond. Asp45, which also serves as a ligand of Zn1, helps to properly orient the hydroxide for attack. In the resulting penta-coordinate transition state, which is stabilized by Arg48, the attacking hydroxide ion and the leaving O3′ occupy apical positions. Zn2 plays a crucial role in activating the phosphate and stabilizing the leaving O3′-oxyanion (Fig. 6). Thus all three zinc ions are essential for catalysis and one could call this a 'three-metal ion' mechanism as opposed to the

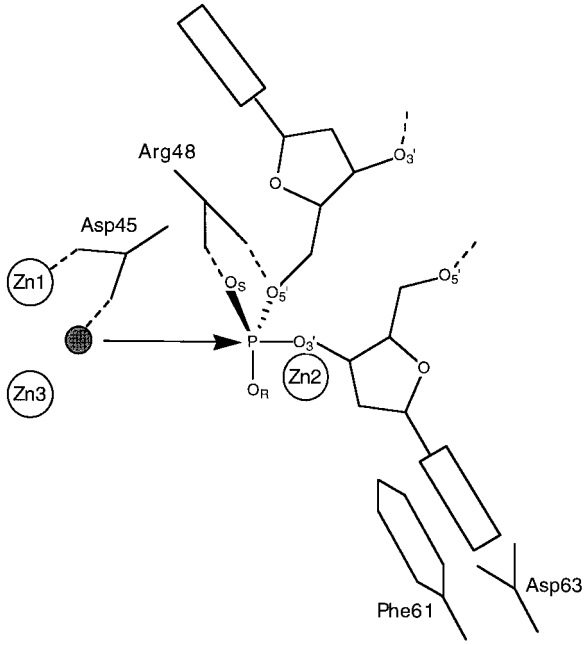

Fig. 6. Proposed catalytic mechanism of P1 nuclease. The hydroxide ion (shaded sphere) bridging Zn1 and Zn3, and properly oriented by Asp45, is attacking the phosphate in-line with the P-O3′-bond. In the resulting penta-coordinated transition state the attacking hydroxide and the leaving O3′ occupy apical positions. Zn2 is stabilizing the leaving O3′-oxyanion, while R48 neutralizes the additional negative charge of the transition state. Steric hindrance between the Rp-sulfur of a phophorothioate or of a phosphorodithioate with Zn2 will prevent cleavage.

'two-metal ion' mechanism proposed for other nucleases (see below).

The catalytic mechanism outlined above is consistent with NMR data showing that P1 hydrolysis proceeds with inversion of configuration at the phosphorus.[5] This mechanism differs in two major aspects from the one considered previously to be most likely on the basis of the 3 Å structure of the P1-(R-Ap(S)A) complex.[10] Firstly, the direction of the oligonucleotide is reversed, i.e. the base 5' to the cleaved bond is now binding in the active site pocket, in agreement with biochemical data.[6–8] Secondly, the hydroxide ion bridging Zn1 and Zn3 rather than one of the water molecules associated with Zn2 is acting as the attacking nucleophile (Fig. 6).

A similar mechanism has been proposed for *B. cereus* phospholipase C (PLC) which has an active site geometry almost identical to that of P1, including the positions of the three water molecules.[11] In a complex with a phosphonate inhibitor of PLC[32] one of the phosphate oxygens was replacing the water bridging Zn1 and Zn3. However, no suitable candidate for the attacking water could be located to suggest that this type of binding would also occur in a productive complex. Simulations by molecular dynamics lead the authors to propose that this complex would only be transient and that the nucleophilic attack at the phosphorus would be carried out by the hydroxide ion bridging Zn1 and Zn3.[15]

In the two-metal ion mechanism originally proposed by Steitz and coworkers for the 3′,5′-exonuclease activity of *E. coli* polymerase I[16] and later also for catalytic RNA and for alkaline phosphatase,[17,33] a free phosphate oxygen is replacing the solvent molecule bridging the two metal ions. One of the metal ions is activating the attacking nucleophile, while the other is stabilizing the leaving O3′-oxyanion. Modelling of such a transition state complex for nuclease P1 is difficult, if not impossible, due to severe steric hindrance and/or the lack of a water molecule in a position suitable for nucleophilic attack. Moreover, this type of complex is definitely not compatible with a hydrogen bonding interaction of the 5′-base with Asp63 which we consistently observe in our complexes and which appears to be an important element of substrate binding by nuclease P1. It should be noted here also, that the distance between the two metal ions is considerably shorter in P1 and PLC (3.2 Å) than in 3′,5′-exonuclease (3.9 Å). It therefore appears unlikely that a two-metal ion mechanism is operating in nuclease P1.

Comparison With Nuclease S1

Nuclease S1 from *Aspergillus oryzae* is highly homologous to nuclease P1 (49.3% sequence identity)[13] and their three-dimensional structures are closely related (I.Törö and D. Suck, unpublished results). The enzymes have similar biochemical properties including the requirement for three zinc ions, although quantitative differences exist in their pH optima and substrate preferences.[34] All the zinc ligands, as well as Phe61 and Asp63 (P1 numbering) at the active site binding pocket are conserved in S1. On the other hand, Arg48 is replaced by a lysine and it is interesting to note that a lysine residue was shown to be essential for activity and possibly involved in substrate binding by S1 suggesting that these residues have similar functions.[35] Surprisingly, residues Tyr144, Asp146, and Tyr155 which form the Tyr-site in nuclease P1 are not conserved and are replaced by Glu, Asn, and Thr, respectively in S1. The non-conservation of this site in S1 nuclease is puzzling and raises the question of the relevance of the Tyr-site for hydrolysis. The structures of P1 in complex with ss-DNA clearly demonstrated its role in nucleotide binding, but they do not provide a convincing explanation for its general function. One could speculate that this secondary site might be involved in destabilization of double-stranded substrates and thus explain the higher activity of P1 towards double-stranded substrates.[2, 36–37]. Mutations of Arg48, Asp63, Asp146, and both Tyr144 and Tyr155 as well as cocrystallization experiments with nuclease S1 could possibly help in answering these questions.

ACKNOWLEDGMENT

Roberto Dominguez was supported by a DAAD fellowship.

REFERENCES

1. Fujimoto, M., Kuninaka, A., Yoshino, H. Identity of phosphodiesterase and phosphomonoesterase activities with nuclease P1. Agr. Biol. Chem. 38:785–790, 1974.
2. Fujimoto, M., Kuninaka, A., Yoshino, H. Substrate specificity of nuclease P1. Agr. Biol. Chem. 38:1555–1561, 1974.
3. Fujimoto, M., Fujiyama, K., Kuninaka, A., Yoshino, H. Mode of action of nuclease P1 on nucleic acids and its specificity for synthetic phosphodiesters. Agr. Biol. Chem. 38:2141–2147, 1974.
4. Fujimoto, M., Kuninaka, A., Yoshino, H. Some physical and chemical properties of nuclease P1. Agr. Biol. Chem. 39: 1991–1997, 1975.
5. Potter, B.V.L., Conolly, B.A., Eckstein, F. Synthesis and configurational analysis of a dinucleoside phosphate isotopically chiral at phosphorus. Stereochemical course of *Penicillium citrinum* nuclease P1 reaction. Biochemistry 22:1369–1377, 1983.
6. Weinfeld, M., Liuzzi, M., Paterson, M.C. Selective hydrolysis by exo- and endonucleases of phosphodiester bonds adjacent to an apurinic site. Nucleic Acids Res. 17:3735–3745, 1989.
7. Weinfeld, M., Soderlind, K.J.M., Buchko, G.W. Influence of nucleic acid base aromaticity on substrate reactivity with enzymes acting on single-stranded DNA. Nucleic Acids Res. 21:621–626, 1993.
8. Box, H.C., Budzinski, E.E., Evans, M.S., French, J.B., Maccubin, A.E. The differential lysis of phosphoester bonds by nuclease P1. Biochim. Biophys. Acta 1161:291–294, 1993.
9. Lahm, A., Volbeda, A., Suck, D. Crystallisation and preliminary crystallographic analysis of P1 nuclease from *Penicillium citrinum*. J. Mol. Biol. 215:207–210, 1990.
10. Volbeda, A., Lahm, A., Sakiyama, F., Suck, D. Crystal structure of *Penicillium citrinum* P1 nuclease at 2.8 Å resolution. EMBO J. 10:1607–1618, 1991.

11. Hough, E., Hansen, L.K., Birknes, B. et al. High-resolution (1.5 Å) of phospholipase C from *Bacillus cereus*. Nature 338:357–360, 1989.
12. Eckstein, F. Nucleoside phosphorothioates. Ann. Rev. Biochem. 54:367–402, 1985.
13. Iwamatsu, A., Aoyama, H., Dibo, G., Tsunasawa, S., Sakiyama, F. Amino acid sequence of nuclease S1 from *Aspergillus oryzae*. J. Biochem. 110:151–158, 1991.
14. Vallee, B.L., Auld, D.S. New perspective on zinc biochemistry: Cocatalytic sites in multi-zinc enzymes. Biochemistry 32:6493–6500, 1993.
15. Sundell, S., Hansen, S., Hough, E. A proposal for the catalytic mechanism in phospholipase C based on interaction energy and distance geometry calculations. Protein Eng. 7:571–577, 1994.
16. Beese, L.S., Steitz, T.A. Structural basis for the 3′-5′ exonuclease activity of *Escherichia coli* DNA polymerase I: A two metal ion mechanism. EMBO J. 10:25–33, 1991.
17. Steitz, T.A., Steitz, J.A. A general two-metal-ion mechanism for catalytic RNA. Proc. Natl. Acad. Sci., U.S.A. 90:6498–6502, 1993.
18. Dahl, B., Bjergårde, K., Nielsen, J., Dahl, O. Deoxynucleoside phosphorodithioates. Preparation by a triester method. Tetrahedron Lett. 31:3489–3492, 1990.
19. Kabsch, W. Evaluation of single-crystal X-ray diffraction data from a position-sensitive detector. J. Appl. Crystallogr. 21:916–924, 1988.
20. Navaza, J. AMoRe: an automated package for molecular replacement. Acta Crystallogr. A50:157–163, 1994.
21. Brünger, A.T. X-PLOR, Version 3.1. New Haven: Yale University Press, 1992.
22. Engh, R.A., Huber, R. Accurate bond and angle parameters for X-ray protein structure refinement. Acta Crystallogr. A47:392–-400, 1991.
23. Brünger, A.T. Free R value: A novel statistical quantity for assessing the accuracy of crystal structures. Nature 355: 472–475, 1992.
24. Roussel, A., Cambillau, C. TURBO-FRODO, CNRS-LCCMB, Marseille, 1992.
25. Laskowski, R.A., McArthur, M.W., Moss, D.S., Thornton, J.M. PROCHECK: a program to check the stereochemical quality of protein structures. J. Appl. Crystallogr. 26:283–291, 1993.
26. Nagai, K. RNA-protein complexes. Curr. Opin. Struct. Biol. 6:53–61, 1996.
27. Suck, D. Common fold, common function, common origin ? Nat. Struct. Biol. 4:161–165, 1997.
28. Bochkarev, A., Pfuetzner, R.A., Edwards, A.M., Frappier, L. Structure of the single-stranded-DNA-binding domain of replication protein A bound to DNA. Nature 385:176–181, 1997.
29. Saenger, W., Suck, D., Eckstein, F. On the mechanism of ribonuclease A. Eur. J. Biochem. 46:559–567, 1974.
30. Wilcox, D.E. Binuclear metallohydrolases. Chem. Rev. 96:2435–2458, 1996.
31. Sträter, N., Lipscomb, W.N., Klabunde, T., Krebs, B. Enzymatische Acyl- und Phosphoryltransferreaktionen unter Beteiligung von zwei Metallionen. Angew. Chem. 108:2158–2191, 1996.
32. Hansen, S., Hough, E., Svensson, L.A., Wong, Y.L., Martin, S.F. Crystal structure of phospholipase C from *Bacillus cereus* complexed with a substrate analog. J. Mol. Biol. 234:179–187, 1993.
33. Kim, E.E., Wyckoff, H.W. Reaction mechanism of alkaline phosphatase based on crystal structures. Two-metal ion catalysis. J. Mol. Biol. 218:449–464, 1991.
34. Linn, S.M., Lloyd, R.S., Roberts, R.J. (eds.). Fungal and mitochondrial nucleases. In: "Nucleases." 2nd edit. New York: Cold Spring Harbor Laboratory Press, 1993:171–207.
35. Gite, S., Reddy, G., Shankar, V. Active site characterization of S1 nuclease. Biochem. J. 285:489–494, 1992.
36. Vogt, V.M. Purification and further properties of single-strand specific nuclease for *Aspergillus oryzae*. Eur. J. Biochem. 33:192–200, 1973.
37. Vogt, V.M. Purification and properties of S1 nuclease from Aspergillus. In: "Methods in Enzymology." Vol. 65. Grossman, L., Moldave, K. (eds.). New York: Academic Press, 1980:248–255.